

# Microstructure and dielectric properties of Nd doped $\text{CaCu}_3\text{Ti}_4\text{O}_{12}$ synthesized by sol–gel method

Mao-Hua Wang · Bo Zhang · Fu Zhou ·  
Chao Yao

Received: 11 September 2013 / Accepted: 11 November 2013 / Published online: 19 November 2013  
© Springer Science+Business Media New York 2013

**Abstract**  $\text{Ca}_{(1-3x/2)}\text{Nd}_x\text{Cu}_3\text{Ti}_4\text{O}_{12}$  ( $x = 0, 0.1, 0.2$  and  $0.3$ ) powders and ceramics were prepared by sol–gel method. Effect of Nd on microstructure and dielectric properties were investigated. XRD patterns suggest that pure perovskite-like CCTO phase were obtained after calcining at  $800^\circ\text{C}$  for 2 h. SEM pictures reveal that particle size monotonously decreases from 250 to 120 nm with increase of Nd concentration. The lattice parameters show an increasing trend with the enhancing amount of  $\text{Nd}^{3+}$  substitution. The average grain size of CCTO ceramics decrease from 2.0 to  $0.8\ \mu\text{m}$  with increase in Nd doping, which indicates that high concentration of Nd inhibits grain growth of  $\text{CaCu}_3\text{Ti}_4\text{O}_{12}$ . Both of the dielectric constant and dielectric loss decrease with increase in Nd concentrations.  $\text{Ca}_{(1-3x/2)}\text{Nd}_x\text{Cu}_3\text{Ti}_4\text{O}_{12}$  ceramics with  $x = 0.3$  shows the lowest dielectric constant of  $1.12 \times 10^4$  as well as the lowest dielectric loss value of 0.12 at  $20^\circ\text{C}$  (10 kHz).

**Keywords**  $\text{CaCu}_3\text{Ti}_4\text{O}_{12}$  · Doping · Nd · Dielectric properties

## 1 Introduction

High dielectric constant materials are useful for miniaturization of electronic devices. In this situation, calcium copper titanate ( $\text{CaCu}_3\text{Ti}_4\text{O}_{12}$ ) has attracted a lot of interest in the past few years. This material exhibits colossal dielectric constant of  $\epsilon_r \sim 10,000$  with the temperature range  $100\text{--}600\ \text{K}$  [1–3]. Temperature independent colossal dielectric constant of  $\text{CaCu}_3\text{Ti}_4\text{O}_{12}$  (CCTO) has drawn the attention of many researchers worldwide. But high dielectric loss ( $\tan\delta$ ), low breakdown voltage and high leakage current have certainly become a barrier to its industrial applications [4]. Among the previous works, the internal barrier layer capacitor (IBLC) model, which considers CCTO as consisting of semi-conducting grains with insulating grain boundaries, has been widely accepted to describe the origin of the unusually high dielectric constant of CCTO [5–7]. This electrostatic barrier obstacles the current flow through the bulk semi-conducting grains in presence of an applied field resulting huge dielectric constant value.

It is known that the radius, valency and coordination number of an element are important parameters to determine the site it occupies in the parent compound. Up to now, there are several reports on the giant dielectric properties of CCTO [8, 9] and related oxides of the type  $\text{ACu}_3\text{Ti}_4\text{O}_{12}$  where  $A = \text{Sr}$  [10],  $\text{Cd}$  [11, 12],  $\text{La}_{2/3}$  [13, 14]. Some doping ions can reduce significantly dielectric loss of CCTO ceramics.  $\text{La}^{3+}$  substitution into CCTO can reduce dielectric loss to be less than 0.03 [15]. Both Nb and Fe doping lowered the dielectric loss [16]. The dielectric loss at low frequencies ( $f < 10^4\ \text{Hz}$ ) in  $\text{CaCu}_3\text{Ti}_4\text{O}_{12}$  could be reduced by adding  $\text{CaTiO}_3$  and  $\text{ZrO}_2$  [17, 18]. However, the reduction of dielectric loss is usually accompanied by a decrease in dielectric

M.-H. Wang · B. Zhang (✉) · F. Zhou · C. Yao  
Jiangsu province Key Laboratory of Fine Petrochemical  
Industry, Changzhou University, Changzhou 213164,  
Jiangsu, People's Republic of China  
e-mail: bozh5237269@163.com

M.-H. Wang · B. Zhang · F. Zhou · C. Yao  
School of Chemistry and Chemical Engineering, Changzhou  
University, Changzhou 213164, Jiangsu, People's Republic of  
China

constant value. Dielectric loss of CCTO is too high due to conducting crystalline grains/sub grains. The conductance of the barrier leads to the leakage loss. It has been revealed that addition of  $\text{CaTiO}_3$  increases the resistance of the barrier layers [19, 20].

CCTO was generally prepared by the traditional solid-state method [1], which suffers from the disadvantages of tedious work, relatively long reaction times, high calcined temperatures and inhomogeneity [21]. In recent years, there were a lot of reports on the sol–gel processing to synthesize CCTO [22–24]. Compared with traditional solid-state method, the sol–gel method affords intimate and homogeneous mixing of the metal ions at the molecular scale, thus reducing the diffusion path length required. Shorter diffusion lengths lead to shorter reaction times and lower temperatures [23]. In addition, many different processing conditions can be selected in the sol–gel technique, such as reagent, solvent, temperature, etc. In this work, an attempt has been made to synthesize a few compositions in the  $\text{Ca}_{(1-3x/2)}\text{Nd}_x\text{Cu}_3\text{Ti}_4\text{O}_{12}$  (CNCTO) by sol–gel method and study its microstructure and dielectric properties.

## 2 Experimental

All of employed chemicals were analytical reagent grade and supplied by ShangHai LingFeng Chemical Reagent Co. Ltd.  $\text{Ca}_{(1-3x/2)}\text{Nd}_x\text{Cu}_3\text{Ti}_4\text{O}_{12}$  ( $x = 0, 0.1, 0.2$  and  $0.3$ , designated as CCTO, CNCTO<sub>1</sub>, CNCTO<sub>2</sub> and CNCTO<sub>3</sub>, respectively) powders were prepared by sol–gel method. The weighted  $\text{Ca}(\text{NO}_3)_2 \cdot 4\text{H}_2\text{O}$ ,  $\text{Cu}(\text{NO}_3)_2 \cdot 3\text{H}_2\text{O}$  and  $\text{Nd}(\text{NO}_3)_3 \cdot 6\text{H}_2\text{O}$  were dissolved into absolute ethyl alcohol and deionize water (the volume ratio of absolute ethyl alcohol to water = 3:1). Meanwhile, stoichiometric  $\text{Ti}(\text{OC}_4\text{H}_9)_4$  liquids were dissolved into  $\text{CH}_3\text{CH}_2\text{OH}$  to form 0.5 M solution. Acetic acid was added to adjust the acidity of solution (pH 3) in order to form the gels slowly. Both above solutions were mixed with vigorous stirring. Amount of citric acid was added into the mixture and the blue gel was gradually formed. Subsequently, the gel was dried at 80 °C to obtain xerogels. Finally, the xerogels was calcined at 800 °C for 2 h to yield  $\text{Ca}_{(1-3x/2)}\text{Nd}_x\text{Cu}_3\text{Ti}_4\text{O}_{12}$  powders.

The as-prepared powders were thoroughly pulverized in an agate mortar and pressed into discs of 10 mm in diameter at around 50 MPa and sintered at 1,000 °C for 6 h. After polishing, silver paste was used to coat both sides of sintered discs, and then fired at 600 °C for 10 min to form electrodes in order to measure dielectric properties.

The thermal decomposition characteristic of xerogel was investigated by TG/DSC (TG 209 F3, Germany) in air

atmosphere with heating rate of 10 °C/min from 30 to 800 °C. The phase composition of the powders and the sintered ceramics were analyzed by X-ray powder diffraction (D/max 2,500 PC, Japan) using a  $\text{Cu K}\alpha$  radiation ( $\lambda = 0.15406$  nm) from 20 to 80°. The microstructure of powders and ceramics was observed using SEM (JSM-6360LA, Japan) and energy dispersive spectroscopy (JSM-6360LA, Japan). The relative density of ceramics was measured by the Archimedes method. Dielectric properties of sintered ceramics were measured as a function of temperature using a LCR meter (AT821, China).

## 3 Results and discussion

TG/DSC was carried out on xerogel to study the thermal decomposition process. Figure 1 shows the representative TG/DSC plots of the precursor of  $\text{Ca}_{(1-3x/2)}\text{Nd}_x\text{Cu}_3\text{Ti}_4\text{O}_{12}$  with  $x = 0.2$ . It is observed that there are three stages of weight loss corresponding to an endothermic peak and two exothermic peaks in the temperature range up to 700 °C. The DSC curve appears a small endothermic peak at 192 °C, accompanied by about 26.6 % weight loss in TG curve, which resulted from the removal of absorbed water and solvent. At the elevating temperature, two exothermic peaks appear at 247 and 295 °C in DSC curve, accompanied by 15.9 and 7.7 % weight loss in TG curve, respectively, which may be due to the main decomposition of nitrates and organic groups. There is almost no weight loss in TG curve above 400 °C, which indicates non-crystalline oxides slowly reacted and transferred to polycrystallines.

To help understand the evolution of the powders, XRD patterns of  $\text{Ca}_{(1-3x/2)}\text{Nd}_x\text{Cu}_3\text{Ti}_4\text{O}_{12}$  for ( $x = 0.2$ ) xerogels with different heat-treatment temperatures are shown in

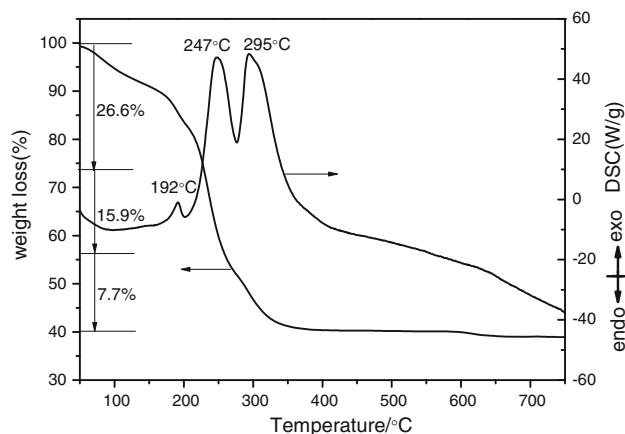


**Fig. 1** TG/DSC plot of  $\text{Ca}_{(1-3x/2)}\text{Nd}_x\text{Cu}_3\text{Ti}_4\text{O}_{12}$  for ( $x = 0.2$ )

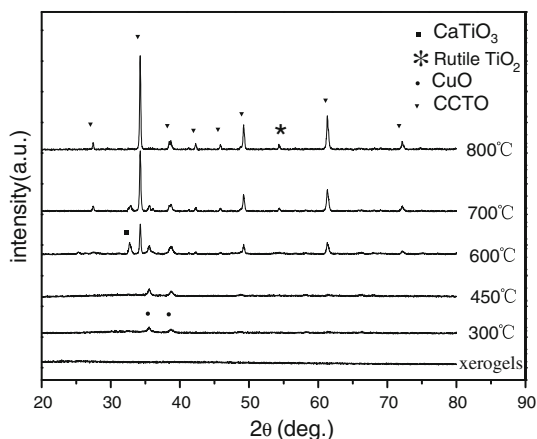


**Fig. 2** XRD patterns of CNCTO<sub>2</sub> xerogels with different heat-treatment temperatures

Fig. 2. It can be seen in the figure that xerogels are amorphous without heat-treatment. The powders calcined at 300 °C shows the peaks corresponding to CuO. The diffraction peaks corresponding CCTO crystalline

gradually appear and small amount of CaTiO<sub>3</sub> and CuO are also present in this stage when the calcination temperature increases to 600 °C. With the increase in the calcination temperature from 600 to 800 °C, the peaks of CCTO increase in intensity and the peaks corresponding to CuO and CaTiO<sub>3</sub> decrease and vanish completely when the calcinations temperature is 800 °C. This indicates that CaTiO<sub>3</sub> react with CuO to form CCTO powders above 600 °C. And we observed a small amount of rutile TiO<sub>2</sub> phase formation at 800 °C. No secondary phases containing Nd were detected because XRD is not sensitive to concentrations under 0.5 wt% [25]. The Nd<sup>3+</sup> was most likely substituted in Ca lattice sites. These two occurrences are attributed to the lack of Nd found in the CNCTO<sub>2</sub> XRD spectra.

Figure 3 shows SEM photographs of pure and Nd doped CCTO powders at various levels after calcining at 800 °C for 2 h. SEM observation indicates that all samples exhibit a good dispersity with uniform particle size. It decreases to 120 nm for  $x = 0.3$ , from 250 nm for  $x = 0$ . It can be assumed that Nd has effect on CCTO particle size.

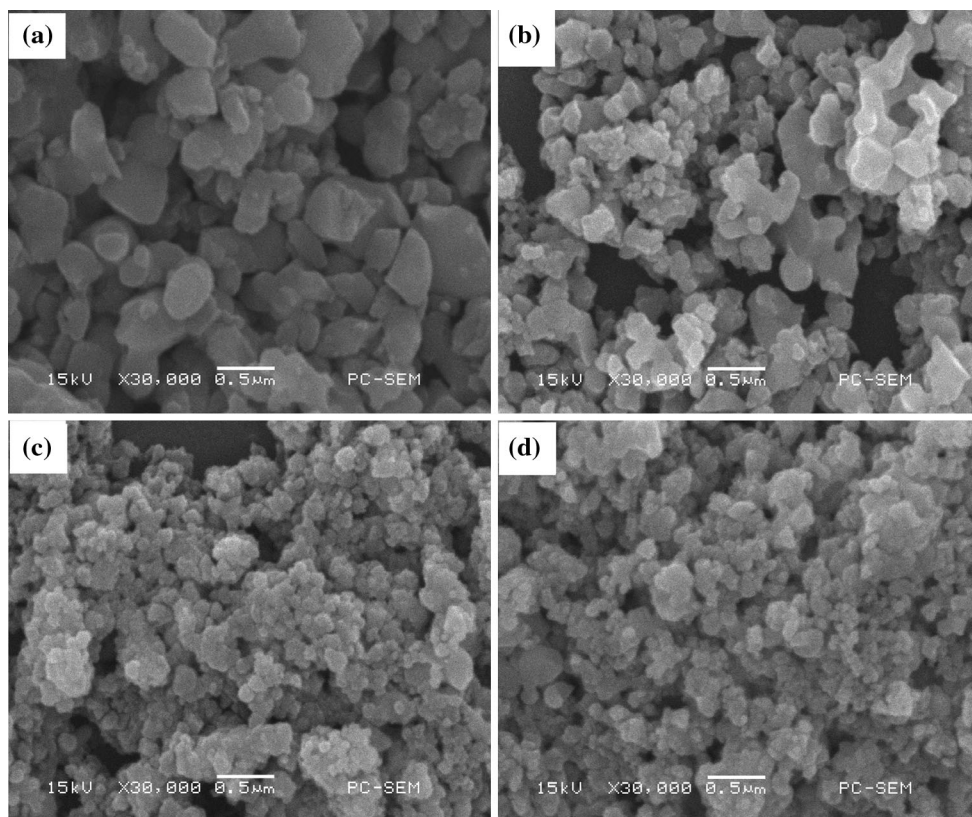


**Fig. 3** SEM photographs of **a** CCTO, **b** CNCTO<sub>1</sub>, **c** CNCTO<sub>2</sub>, **d** CNCTO<sub>3</sub> powders

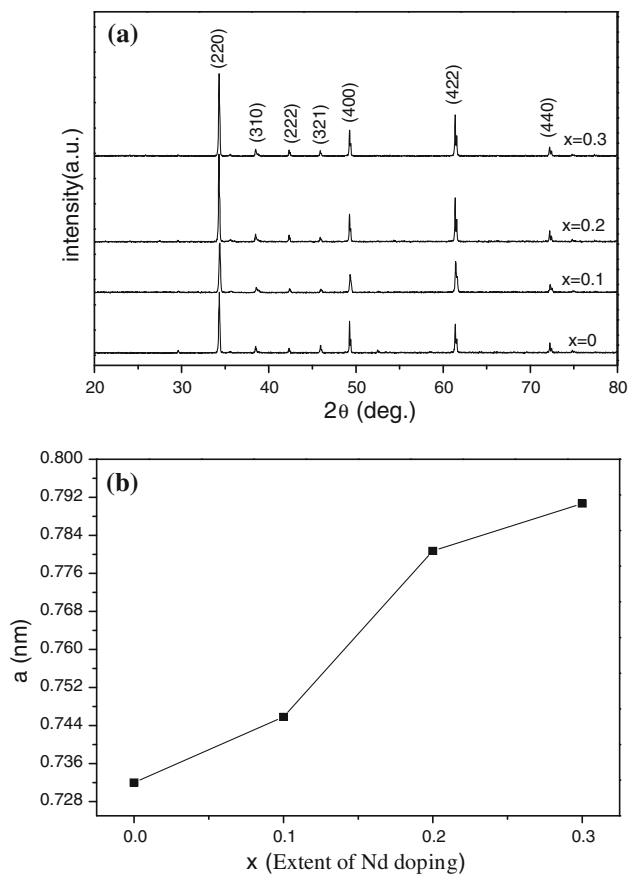


**Fig. 4** **a** X-ray diffraction pattern of  $\text{Ca}_{(1-3x/2)}\text{Nd}_x\text{Cu}_3\text{Ti}_4\text{O}_{12}$  ceramics, **b** Variation of lattice parameters with the extent of Nd doping

Meanwhile, the particle size decreases with increase in dopant concentration, also reported by other authors for sol-gel methods [14].

X-ray diffraction patterns of  $\text{Ca}_{(1-3x/2)}\text{Nd}_x\text{Cu}_3\text{Ti}_4\text{O}_{12}$  (where  $x = 0, 0.1, 0.2$  and  $0.3$ ) ceramics are shown in Fig. 4. Comparing these patterns with those of the standard powder XRD pattern of CCTO (JCPDS Card No.75–2188), the diffractogram shows that the sintered ceramics are polycrystalline and no secondary phase is formed for doping by Nd up to  $x = 0.3$ , leading to conclude that  $\text{Nd}^{3+}$  is replacing  $\text{Ca}^{2+}$  in its lattice position in the doped ceramics, without distorting the crystal structure. The lattice parameter was determined using least square refinement method show an increasing trend with the enhancing amount of  $\text{Nd}^{3+}$  substitution. It increases to 0.73907 nm for  $x = 0.3$ , from 0.7320 nm for  $x = 0$ . This lattice parameter enhancement with increasing amount of  $\text{Nd}^{3+}$  doping is expected since the ionic size neodymium ( $\text{Nd}^{3+}$ ) is bigger than that of calcium ( $\text{Ca}^{2+}$ ). This is called ionic size effect. Researchers have proved the existence of  $\text{Ti}^{3+}$

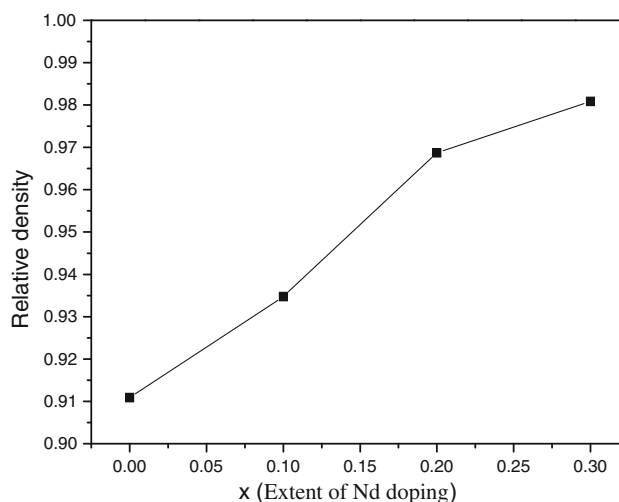


**Fig. 5** Relative density of pure and Nd doped CCTO ceramics sintered at 1,000 °C for 6 h

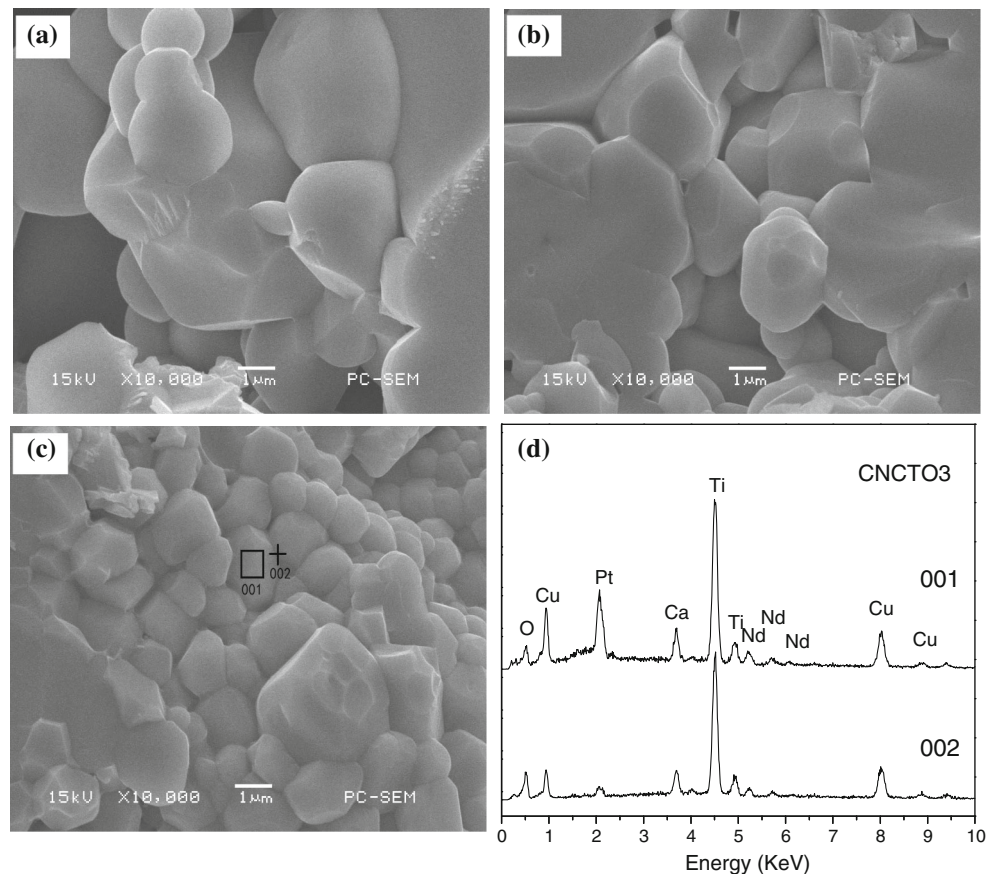
along with  $\text{Ti}^{4+}$  from the photoemission spectroscopy of CCTO [26]. Therefore this reduction of lattice parameter may also be due to increasing amount of  $\text{Ti}^{3+}$ , formed by reduction of  $\text{Ti}^{4+}$  to  $\text{Ti}^{3+}$  by  $\text{Nd}^{3+}$  due to its oxidizing property.

Figure 5 presents the variation of relative density of  $\text{Ca}_{(1-3x/2)}\text{Nd}_x\text{Cu}_3\text{Ti}_4\text{O}_{12}$  ceramics as a function of Nd concentration. It can be seen that the relative densities increase as Nd concentration increase.  $\text{CNCTO}_3$  ceramics shows the highest relative density of 98.1 %, which may be due to less pores and uniform particle size of powders. It is difficult to prepare fully dense ceramics due to a lot of factors which can affect on producing fine-grained materials with high density, such as powder preparation process, powder agglomeration and sintering conditions [27]. In addition, many researchers reported that dopants can also have effect on the densification and microstructure of perovskite [28].

Figure 6a, b, c presents SEM images of fracture surface for pure and Nd doped CCTO ceramics. It is clearly seen that microstructure of  $\text{CNCTO}$  ceramics changes significantly with increase in concentration of Nd. The average grain size becomes small with increase in Nd doping. Pure CCTO shows the average grain size about 2.0  $\mu\text{m}$ , whereas for subsequent doping concentrations, the average grain size decreases to 0.8  $\mu\text{m}$  for  $\text{CNCTO}_3$  ceramics. This result indicates that Nd inhibits grain growth of CCTO ceramics.

Energy spectrum of elemental analysis performed on different regions of  $\text{CNCTO}_3$  gives insight into the proportion of different elements in grain and grain boundary. It can be seen from Fig. 6d that Nd appears in the grain and

**Fig. 6** SEM images of  $\text{Ca}_{(1-3x/2)}\text{Nd}_x\text{Cu}_3\text{Ti}_4\text{O}_{12}$  ceramics: **a**  $x = 0$ , **b**  $x = 0.1$ , **c**  $x = 0.3$ , **d** gives EDS analysis of CNCTO ( $x = 0.3$ ) for different regions



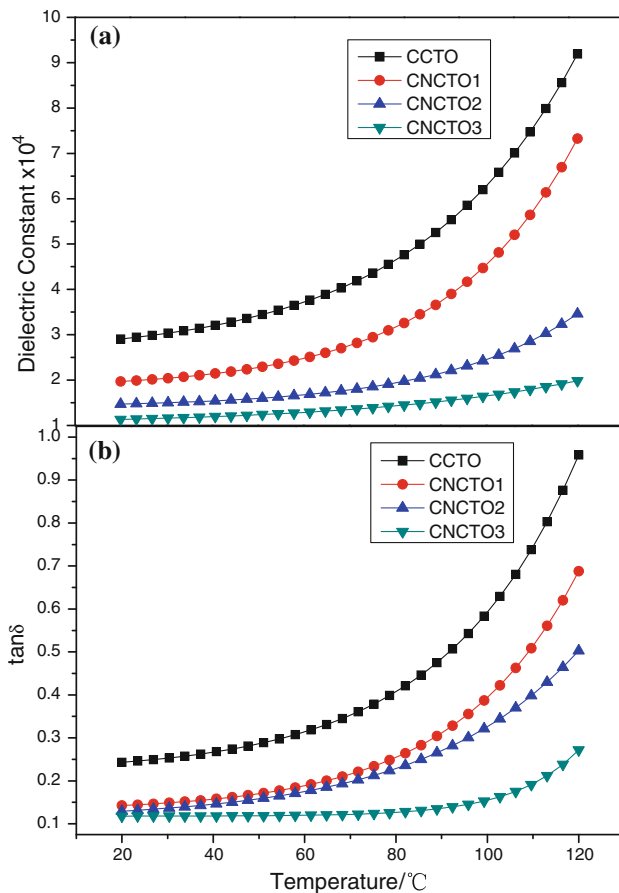
grain boundary of  $\text{CNCTO}_3$  as well as Ca, Cu, Ti, and O (the peaks of Pt were originated for conducting of specimen). Major content of Nd was found in grain (10.99 %) than in grain boundary region (9.57 %). Lesser Nd content in the grain boundary may be the major cause for the refinement in grain size [29].

Figure 7a illustrates temperature dependence of the dielectric properties for pure and Nd doped CCTO ceramics at the frequency of 10 kHz. The dielectric constant ( $\epsilon_r$ ) and dielectric loss ( $\tan\delta$ ) increased continuously by increasing temperature, although the rate of these enhancements was not the same. It can be seen that the thermal stability of  $\text{CNCTO}_2$  and  $\text{CNCTO}_3$  is considerably higher than that of CCTO and  $\text{CNCTO}_1$ . It is obvious that the dielectric constant and dielectric loss was found to drastic decreases with increase in Nd dopant concentration. CCTO exhibits the highest dielectric constant ( $2.9 \times 10^4$ ) and dielectric loss (0.24) at 20 °C, while  $\text{CNCTO}_3$  shows the lowest dielectric constant ( $1.12 \times 10^4$ ) and dielectric loss (0.12) at 20 °C. The results indicate that Nd doping can decrease dielectric constant as well as dielectric loss. According to the

literature [30], the dielectric constant of  $\text{CaCu}_3\text{Ti}_4\text{O}_{12}$  is closely related to its grain size, and larger grains result in higher dielectric constants for  $\text{CaCu}_3\text{Ti}_4\text{O}_{12}$ . Our results lead to the same conclusion, whereby with larger grain size, a larger dielectric constant was observed for pure CCTO. It can be easily understood with the internal barrier layer capacitor (IBLC) model, which consider materials consist of conducting grains and insulating grain boundaries. As a greater amount of crystal defects are able to exist in larger grains than that in smaller ones. Thus, there must be insulating planar defects in these grains. Dopants frequently concentrate at lattice defects. The Nd may be concentrating on the important planar defects in CCTO. This could increase the electrical resistivity of the internal barrier and decrease the dielectric loss.

#### 4 Conclusion

Sol-gel method was employed to synthesize pure and Nd-doped  $\text{CaCu}_3\text{Ti}_4\text{O}_{12}$  ceramics. XRD patterns shows that



**Fig. 7** Temperature dependence of dielectric properties for  $\text{Ca}_{1-3x}\text{Nd}_x\text{Cu}_3\text{Ti}_4\text{O}_{12}$  ceramics at the frequency of 10 kHz

CNCTO ceramics (sintered at 1,000 °C for 6 h) were single phase with no Cu-rich phase. The lattice parameters show an increasing trend with the enhancing amount of  $\text{Nd}^{3+}$  substitution. SEM graphs show that the particle size decreases with increase of Nd concentration. Dielectric constant and dielectric loss is found to decrease with the increase of Nd incorporation. CNCTO<sub>3</sub> ceramics exhibits the lowest dielectric constant of  $1.12 \times 10^4$  as well as the lowest dielectric loss value of 0.12 at 20 °C (10 k Hz). Nd doping has obvious effects on grain growth and dielectric properties of CCTO ceramics.

**Acknowledgments** This work was financially supported by Chang Zhou Science and technology innovation project (CC20120031). We thank Testing Center of Chang Zhou University for providing facility.

## References

- Subramanian MA, Dong L, Duan N (2000) High dielectric constant in  $\text{ACu}_3\text{Ti}_4\text{O}_{12}$  and  $\text{ACu}_3\text{Ti}_3\text{FeO}_{12}$  phases. *J Solid State Chem* 151:323–325
- Li J, Sleight AW, Subramanian MA (2005) Evidence for internal resistive barriers in a crystal of the giant dielectric constant material:  $\text{CaCu}_3\text{Ti}_4\text{O}_{12}$ . *J Solid State Commun* 135:260–262
- Jin S, Xia H, Zhang Y, Guo J, Xu J (2007) Synthesis of  $\text{CaCu}_3\text{Ti}_4\text{O}_{12}$  ceramic via a sol–gel method. *Mater Lett* 61:1404–1407
- Adams TB, Sinclair DC, West AR (2002) Giant barrier layer capacitance effects in  $\text{CaCu}_3\text{Ti}_4\text{O}_{12}$  ceramics. *Adv Mater* 14:1321–1323
- Kwon S, Huang CC, Subramanian MA, Cann DP (2009) Effects of cation stoichiometry on the dielectric properties of  $\text{CaCu}_3\text{Ti}_4\text{O}_{12}$ . *J Alloys Compd* 473:433–436
- West AR, Adams TB, Morrison FD, Sinclair DC (2004) Novel high capacitance materials:  $\text{BaTiO}_3$ : La and  $\text{CaCu}_3\text{Ti}_4\text{O}_{12}$ . *J Eur Ceram Soc* 24:1439–1448
- Adams TB, Sinclair DC, West AR (2006) Influence of processing conditions on the electrical properties of  $\text{CaCu}_3\text{Ti}_4\text{O}_{12}$  ceramics. *J Am Ceram Soc* 89:3129–3135
- Thongbai P, Putasaeng B, Yamwong T, Maensiri S (2011) Improved dielectric and non-ohmic properties of  $\text{Ca}_2\text{Cu}_2\text{Ti}_4\text{O}_{12}$  ceramics prepared by a polymer pyrolysis method. *J Alloys Compd* 506:7416–7420
- Felix AA, Orlandi MO, Varela JA (2011) Schottky-type grain boundaries in CCTO ceramics. *Solid State Commun* 151:1377–1381
- Xue H, Guan XF, Yua R, Xiong ZX (2009) Dielectric properties and current–voltage nonlinear behavior of  $\text{Ca}_{1-x}\text{Sr}_x\text{Cu}_3\text{Ti}_4\text{O}_{12}$  ceramics. *J Alloys Compd* 482:L14–L17
- Subramanian MA, Sleight AW (2002)  $\text{ACu}_3\text{Ti}_4\text{O}_{12}$  and  $\text{ACu}_3\text{Ru}_4\text{O}_{12}$  perovskites: high dielectric constants and valence degeneracy. *Solid State Sci* 4:347–351
- Zuo R, Feng L, Yan Y, Chen B, Cao G (2006) Observation of giant dielectric constant in  $\text{CdCu}_3\text{Ti}_4\text{O}_{12}$  ceramics. *Solid State Commun* 138:91–94
- Rai AK, Mandal KD, Kumar D, Parkash O (2009) Dielectric properties of lanthanum-doped  $\text{CaCu}_3\text{Ti}_4\text{O}_{12}$  synthesized by semi-wet route. *J Phys Chem Solids* 70:834–839
- Xin LZ, Zhi MM, Zou JX, Guang C (2006) Preparation and characterization on nano-sized barium titanate powder doped with lanthanum by sol–gel process. *J Rare Earth* 24:82–85
- Feng L, Tang X, Yan Y, Chen X, Jiao ZJ, Cao GH (2006) Decrease of dielectric loss in  $\text{CaCu}_3\text{Ti}_4\text{O}_{12}$  ceramics by La doping. *Phys Status Solidi* 203(4):R22–R24
- Grubbs RK, Venturini EL, Clem PG, Richardson JJ, Tuttle BA, Samara GA (2005) Dielectric and magnetic properties of Fe- and Nb-doped  $\text{CaCu}_3\text{Ti}_4\text{O}_{12}$ . *Phy Rev B* 72:104–111
- Kobayashi W, Terasaki I (2005)  $\text{CaCu}_3\text{Ti}_4\text{O}_{12}/\text{CaTiO}_3$  composite dielectrics: Ba/Pb-free dielectric ceramics with high dielectric constants. *Appl Phys Lett* 87:032902–032904
- Patterson EA, Kwon S, Huang CC, Cann DP (2005) Effects of  $\text{ZrO}_2$  additions on the dielectric properties of  $\text{CaCu}_3\text{Ti}_4\text{O}_{12}$ . *Appl Phys Lett* 87:182911–182913
- Kumar Rai A, Mandal KD, Kumar D, Parkash O (2009) Dielectric properties of lanthanum-doped  $\text{CaCu}_3\text{Ti}_4\text{O}_{12}$  synthesized by semi-wet route. *J Phys Chem Solids* 70:834–839
- Guillemet FS, Lebey T, Boulos M, Durand B (2006) Dielectric properties of  $\text{CaCu}_3\text{Ti}_4\text{O}_{12}$  based multiphased ceramics. *J Eur Ceram Soc* 26:1245–1257
- Jha P, Arora P, Ganguli AK (2003) Polymeric citrate precursor route to the synthesis of the high dielectric constant oxide,  $\text{CaCu}_3\text{Ti}_4\text{O}_{12}$ . *Mater Lett* 57:2443–2446
- Deepam M, Devendra PS, Agrawal DC, Mohapatra YN (2008) Preparation of high dielectric constant thin films of  $\text{CaCu}_3\text{Ti}_4\text{O}_{12}$  by sol–gel. *Bull Mater Sci* 31:55–59
- Liu LJ, Fan HQ, Fang PY, Chen XL (2008) Sol–gel derived  $\text{CaCu}_3\text{Ti}_4\text{O}_{12}$  ceramics: synthesis, characterization and electrical properties. *Mater Res Bull* 43:1800–1807
- Sun DL, Wu AY, Yin ST (2008) Structure, properties, and impedance spectroscopy of  $\text{CaCu}_3\text{Ti}_4\text{O}_{12}$  ceramics prepared by sol–gel process. *J Am Ceram Soc* 91:169–173

25. Xu D, Shi LY, Wu ZH, Zhong QD, Wu XX (2009) Microstructure and electrical properties of ZnO–Bi<sub>2</sub>O<sub>3</sub>-based varistor ceramics by different sintering processes. *J Eur Ceram Soc* 29:1789–1794
26. Zhang L, Tang ZJ (2004) Polaron relaxation and variable-range-hopping conductivity in the giant-dielectric-constant material CaCu<sub>3</sub>Ti<sub>4</sub>O<sub>12</sub>. *Phys Rev B* 70:174306–174310
27. Luan W, Gao L, Guo J (1999) Size effect on dielectric properties of fine grained BaTiO<sub>3</sub> ceramics. *Ceram Int* 25:727–729
28. Stojanovic BD, Zaghete MA, Foschini CR, Vieira FOS, Varela JA (2002) Structure and properties of donor doped barium titanate prepared by citrate process. *Ferroelectrics* 270:15–20
29. Kashyapa R, Mishraa RK, Thakurb OP, Tandon RP (2012) Structural, dielectric properties and electrical conduction behavior of Dy substituted CaCu<sub>3</sub>Ti<sub>4</sub>O<sub>12</sub>. *Ceram Int* 38:6807–6813
30. Marchin L, Guillemet-Fritsch S, Durand B, Levchenko AA, Navrotsky A, Lebey T (2008) Grain growth-controlled giant permittivity in soft chemistry CaCu<sub>3</sub>Ti<sub>4</sub>O<sub>12</sub> ceramics. *J Am Ceram Soc* 91:485–489